ASME DESIGN ENGINEERING CONFERENCE & SHOW

1980

78. /
1519
10201

ASME

Design Engineering Conference & Show

1980

C O N T E N T S

THE AMERICAN SOCIETY OF MECHANICAL ENGINEERS
345 E 47 St., New York, N.Y. 10017

The Society shall not be responsible for statements or opinions advanced in papers or discussion at meetings of the Society or of its Divisions or Sections, or printed in its publications. Discussion is printed only if the paper is published in an ASME Journal or Proceedings. Released for general publication upon presentation. Full credit should be given to ASME, the Technical Division, and the author.

Loading Conditions in Bolted and Riveted Joints Affected by Plate Thickness Ratio

H. H. Ziada
Asst. Professor,
King Abdul Aziz University,
Saudi Arabia

A. K. Abd El Latif[1]
Assoc. Professor
King Abdul Aziz University, S.A.

Bolted and riveted connections are quite commonly encountered in various design problems. Many trials have been carried out recently to determine the stress distribution in bolted and riveted joints which is of extreme importance in the design of such joints. Effect of many parameters has been investigated, however effect of thickness ratio of the joint plates did not take too much attention. In this analytic work the effect of various plate thickness on the load and stress distribution in cylindrical bolted joints has been investigated using the finite element technique. Computed results show that the load as well as the stress or pressure distribution under bolt-head or nut are not constant nor uniform. Whatever the thickness ratio of the two plates (L_1/L_2), constant load and stress occurred across the joint under the bolt-head end. Maximum stress on surface and up to the mid plane level showed an increase with the thickness ratio. However the maximum stress on interface decreases with the thickness ratio to reach its lowest at $L_1/L_2 = 1$. End of loading on surface or at mid plane increases with the increase in thickness ratio, and tends to approach a constant value at L_1/L_2 equals 10 or more - on interface the opening position - represented by diameter of joint to bolt diameter D/d, reaches a maximum value of 3.5 then decreases rapidly to reach a constant value of about 2.5 for $L_1/L_2 = 10$ or more. Also the thickness of the plate (L_1) has a pronounced effect on the opening position.

Introduction

When two plates are bolted or riveted together they will be in contact in the immediate vicinity of the bolt-heads and separated beyond it. The determination of pressure distribution and the contact area between bolted plates has been investigated by many workers[1, 2].

Fernland [3], Greenwood [4], and Lardner [5] among others reported solutions based upon the theory of elasticity. These investigators have made use of the Hankel transform method. The basic assumption in their approach is that two bolted plates can be represented by a single plate of the same thickness as the combined thickness of the two plates under the same external loading.

Recent work by the same authors [6] showed that the load as well as the stress depends greatly on the thickness of the joint. Also, the beneficial effect of thickness of the joint on the opening condition has been well established. In all cases investigated, the joint plates were taken of the same thickness. However, the effect of thickness ratio of the joint plates did not take too much attention.

Hence in this work, the effect of plate thickness ratio on the load and stress distribution in cylindrical bolted joints has been investigated using the finite element technique.

[1] On leave from Assiut University, Egypt.

Contributed by the Design Engineering Division for presentation at the Design Engineering Conference and Show, Chicago, Ill., March 24-27, 1980 of the AMERICAN SOCIETY OF MECHANICAL ENGINEERS. Manuscript received at ASME Headquarters Dec. 7, 1978. Paper No. 80-DE-2.

The Finite Element Analysis

One of the most powerful methods of numerical stress analysis presently available is the finite element method [7], [8]. Finite element solutions were used for the analytical study of bolted joints [1], [6]. Fig. 1 shows a typical bolted joint. As a first approach, it is well advised to seek simplifications that retain the basic features of the problem while reducing the complexities as much as possible. Fig. 1(*b*) gives a simple configuration for the joint as axi-symmetric problem.

The model was constructed from two-dimensional isoparametric axi-symmetric ring elements for the plates, bolt and nut. This element type gives considerable improvement in accuracy over the constant strain element [1]. Isotropic linear elastic material behaviour were assumed.

The interfaces between bolt-head, plates and nut were modeled by two dimensional interface element, which represents the physical contact between the two plane surfaces, it may maintain or break the physical contact and allow relative slide to each other. The interface elements are defined by two nodal points on each surface of contact. During solution these interface elements will indicate a normal load if there is contact between the surfaces, and zero load for separation of the two plates. The solution yields a result exactly compatible with the physical model. Thus considerable improvement in accuracy over than that used by other workers.

Fig. 2 shows the finite element model for half of the joint with unequal plate thickness. The interface elements were

Discussion on this paper will be accepted at ASME Headquarters until May 24, 1980

SWTI/1596/05

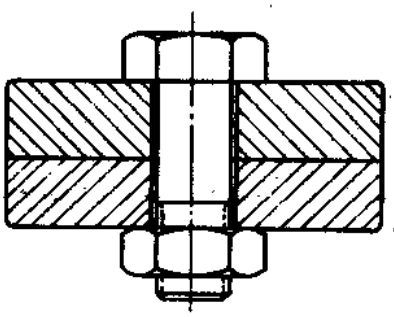

a. bolted joint.

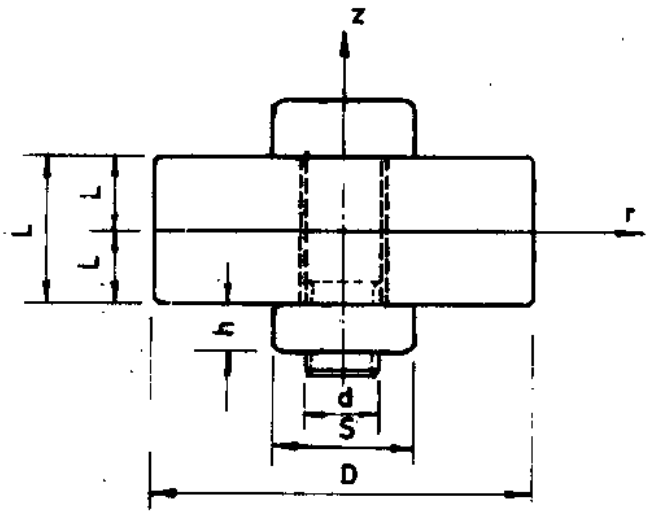

b. simple joint for models

Fig. 1

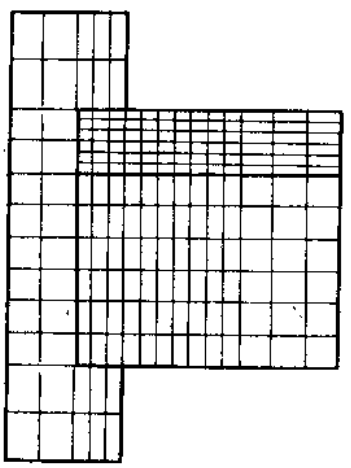

Fig. 2 Finite element model for plates of unequal thickness

given an initial gap of zero magnitude, which resembles the case of contact without preload. Then the load on the bolt and joint was developed by introducing axial displacement at the bolt end. From several solutions with different fixed reference conditions, the nodes along the inside surface of the nut was selected as a fixed reference in the y direction. This condition give similar distributions for the bearing loads under both bolt-head and nut, thus approaching symmetry and simplifying the real conditions. Thus retaining the basic elements of the problem while reducing the complexities as much as possible.

Computations are iterative and the convergence was obtained when the conditions of the interface elements remain unchanged for the last two successive iterations. The material properties for the joint elements, bolt, plates and nut used in the analysis are as follows:

Modulus of elasticity	E	$= 2.1 \times 10^4 \text{MN/mm}^2$
Poissons ratio		$= 0.265$
Density		$= 7800 \text{ Kg/m}^3$
Coefficient of friction for the interface elements		$= 0.75$

Results and Discussion

Computations were performed for joints with total thickness 50mm and plate thickness of: 5 −45, 12.5 −37.5, 20 −30, 25 −25 mms, which corresponds to plate thickness ratio of 9, 3, 1.5, 1, 0.67, 0.33, and 0.11. The plate diameter (D) is 125 mms and diameter of bolt(d) 25mms, $D/d = 5$.

Fig. 3 shows the load distribution on the surface, mid plane, and on interface for the two plates of the joint at various thickness ratio. The maximum load value occurs at the bolt-joint interface under the bearing area of bolt-head. The maximum moves towards the end bolt head as we approach the contact zone or the interface of the joint plates. Whatever the thickness ratio a constant load value occurs across the joint of the end of bolt-head, slight diferences are noticed between distributions occurred on thin and thick plates of each joint.

For comparison purposes, surface, mid plane and interface loads for various thickness ratio are shown in Figs. 4, 5 and 6. The load distribution on the surface is not constant nor uniform as assumed by many workers [1–5]. On mid-plane or interface the end of load occurs at longer radius as the thickness ratio increases. The radius of separation at the contact zone increases with the plate thickness, then decreases.

Fig. 7 summarizes the effect of plate thickness ratio on the end of load at the surface mid plane and interface. On interface the end of load-opening position is greatly affected by the thickness ratio. Opening position or separation radii increases with the increase in L_1/L_2 and reaches to its maximum value of $D/d = 3.5$ at $L_1/L_2 = 1$ then decreases rapidly to approach a constant value of 2.5 for $L_1/L_2 \geq 10$. This result is of considerable importance for design purposes.

Fig. 8, demonstrates that the thickness of the joint plate alone, has also a pronounced effect on the end of load condition. The end of load radii increases with the increase in thickness to diameter ratio (L_1/d). Stresses at the surface, mid plane and interface are shown in Figs. 9, 10 and 11. The stress distribution on the interface is similar to that found recently by Gould and Mikic [1]. The maximum stress value is twice the average value on the bearing area of the bolt-head. Fig. 12, summarized effect of plate thickness ratio on the maximum stress. Generally the maximum stress increases as the thickness ratio increases. At the end close to the interface, the maximum stress decreases with the thickness ratio to reach its lower value at $L_1/L_2 = 1$.

This result is very useful in design, thus an optimum design of bolted joint is achieved primarly by taking joint plates of equal thickness, in which the desired loading is obtained accompanied by minimum stresses and large opening condition.

Fig. 13 shows the effort area-boundary of end of loading across the joint-thickness for various thickness ratio. It is clear that the effort area increases with the increase in

此为试读,需要完整PDF请访问: www.ertongbook.com

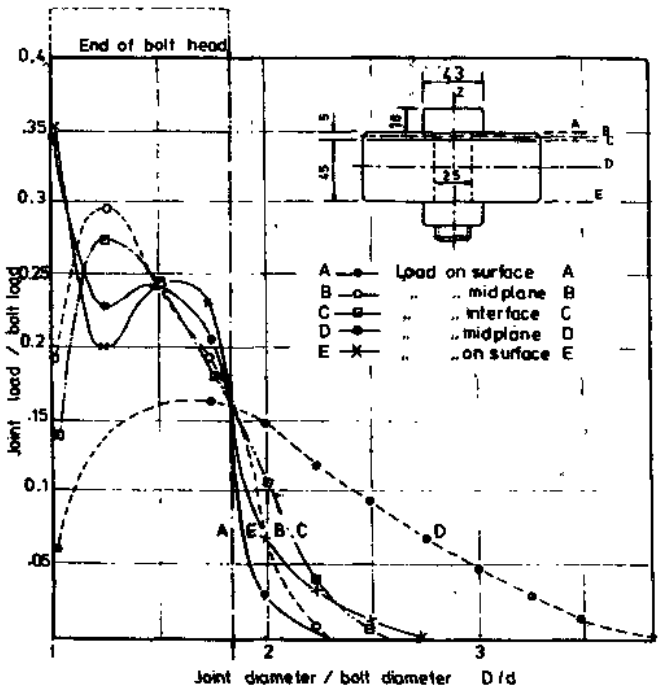

Fig. 3(a) Load distribution along joint length for plate thickness ratio 9

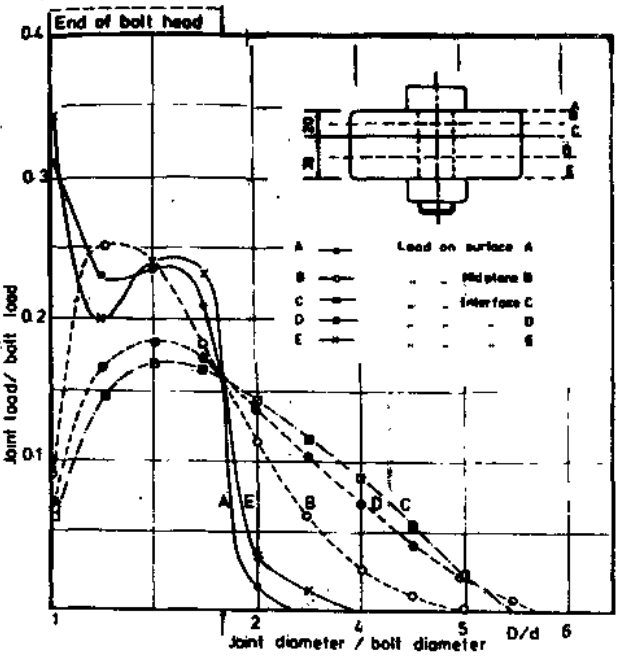

Fig. 3(c) Load distribution along joint length for plate thickness ratio 1.67

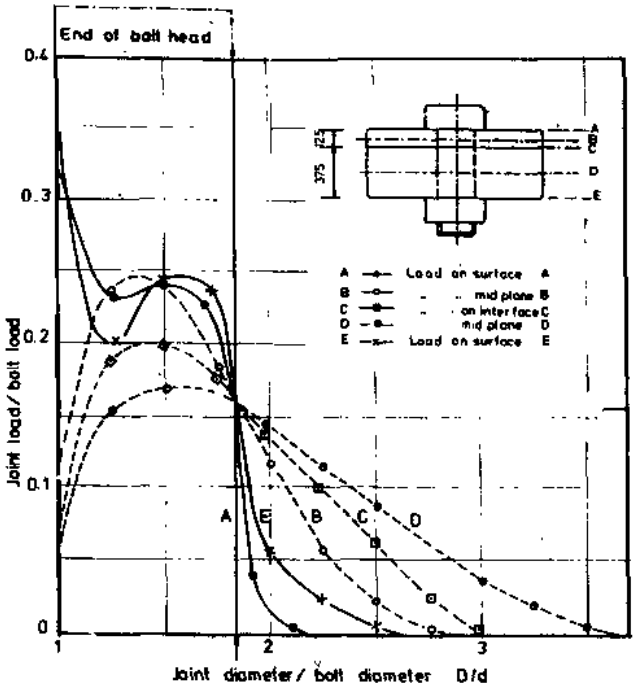

Fig. 3(b) Load distribution alorig joint length for plate thickness ratio 3

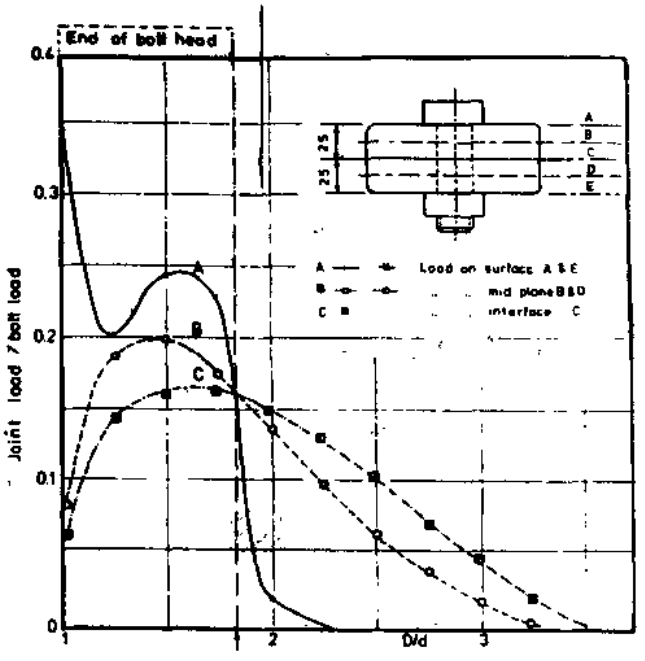

Fig. 3(d) Load distribution along joint length in equal plate thickness

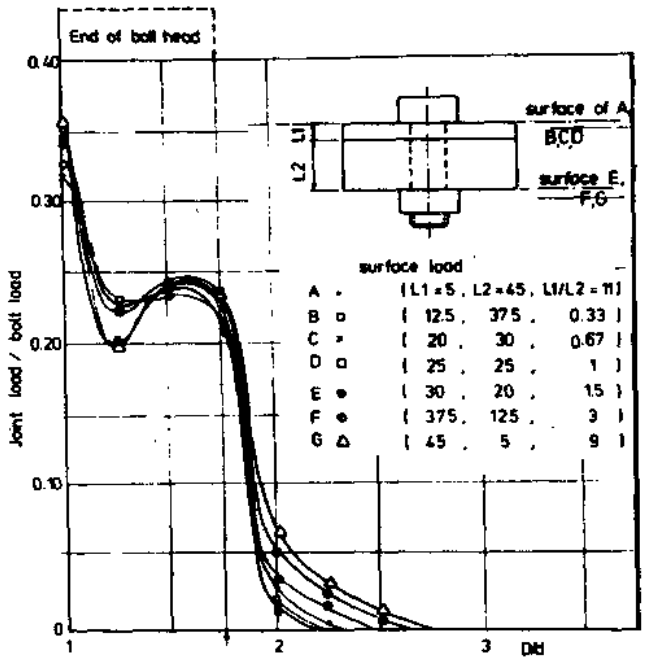

Fig. 4 Load distribution along surface of joints with various thickness ratio

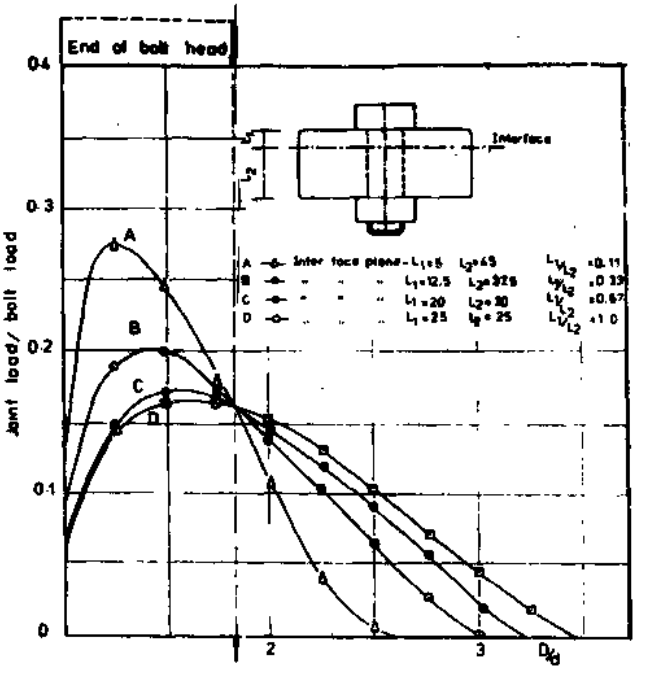

Fig. 6 Load distribution along interface of joints with various thickness ratio

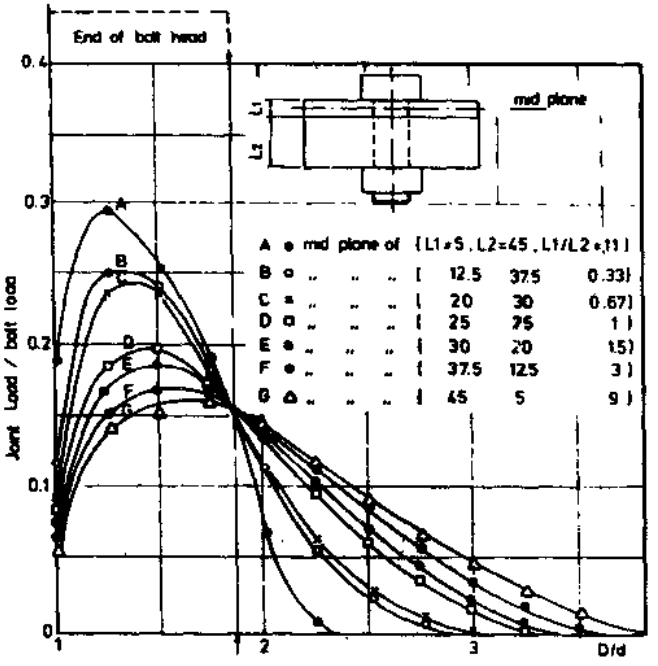

Fig. 5 Load distribution along mid plane of joints with various thickness ratio

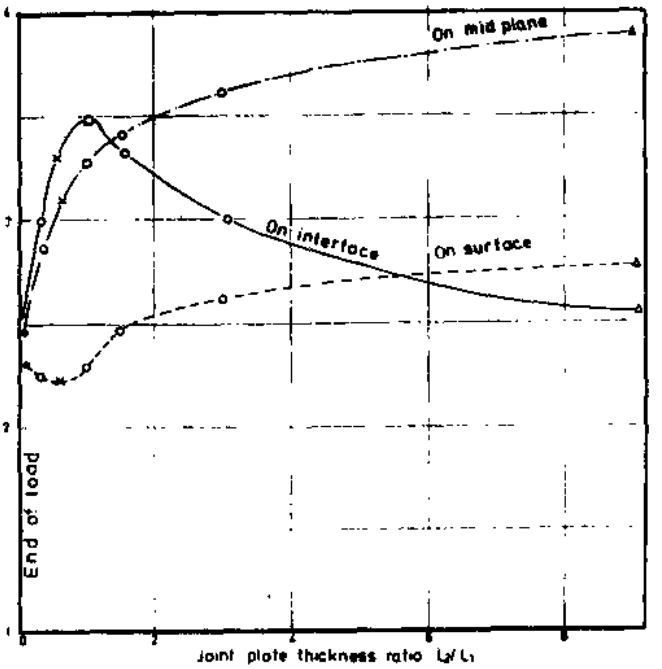

Fig. 7 Effect of joint plate thickness ratio on the end of load

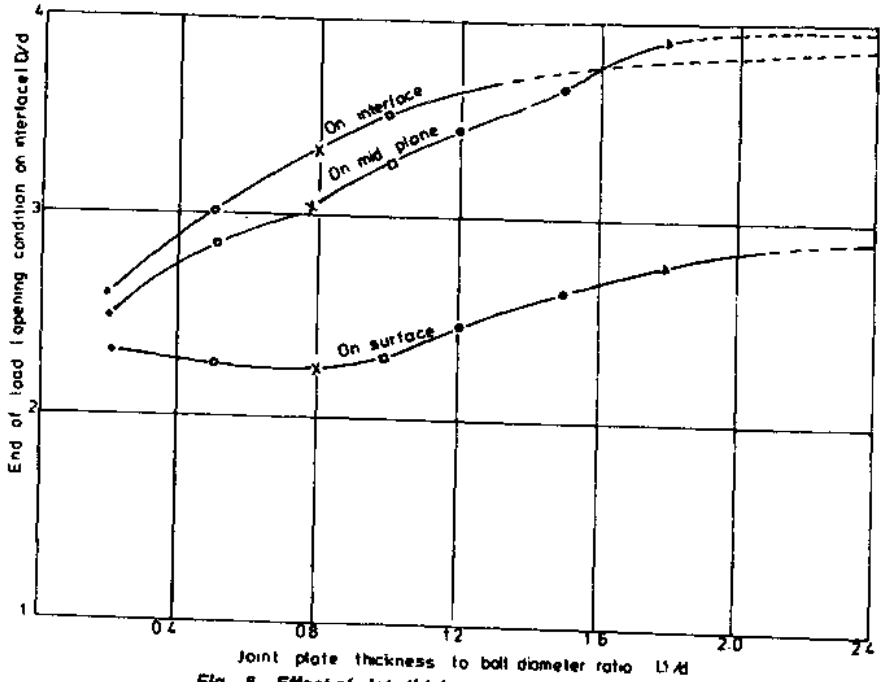

Fig. 8 Effect of plate thickness (L1) on the end of load

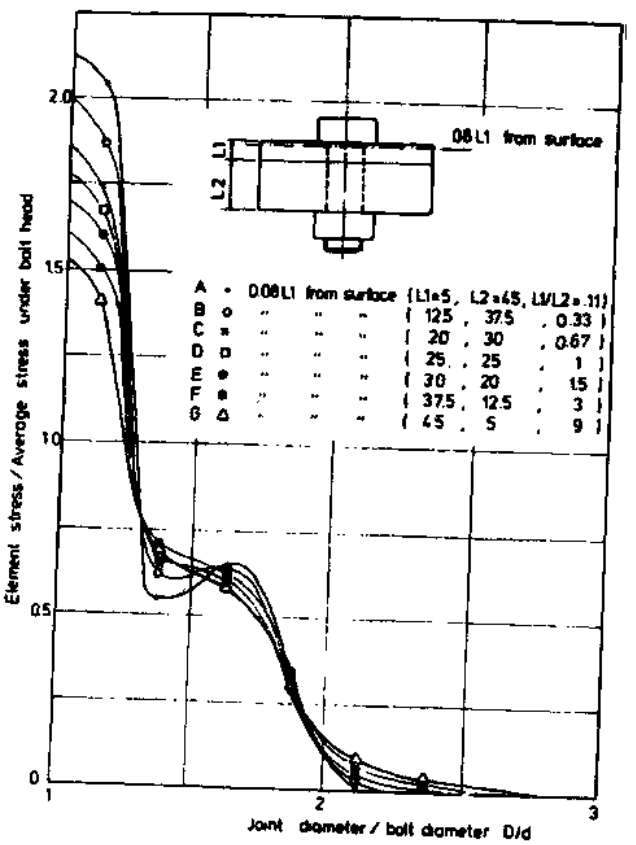

Fig. 9 Stress distribution along joint plate (at .08L from surface)

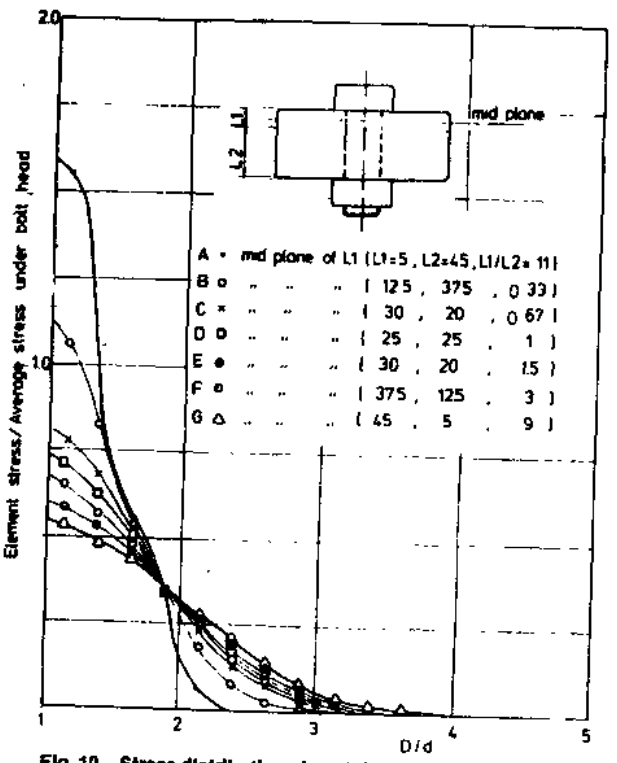

Fig. 10 Stress distribution along joint plate at mid plane

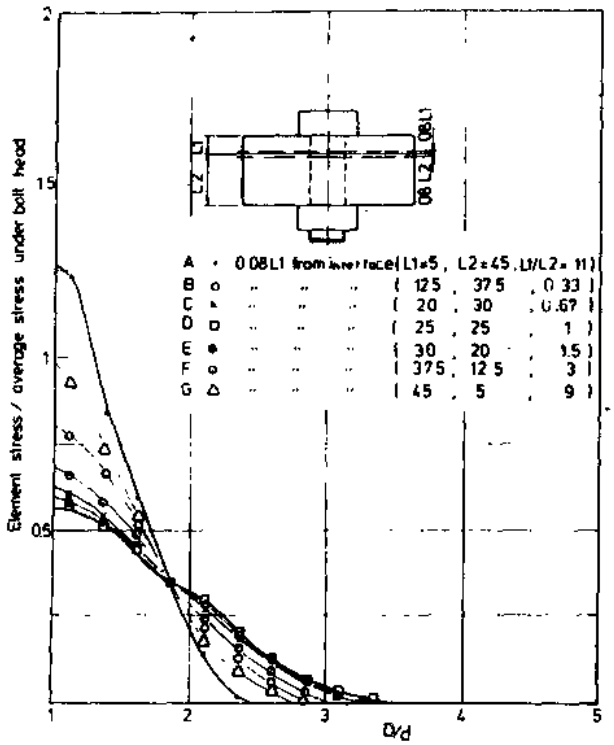

Fig. 11 Stress distribution near to interface (at .08L from interface and along joint plate)

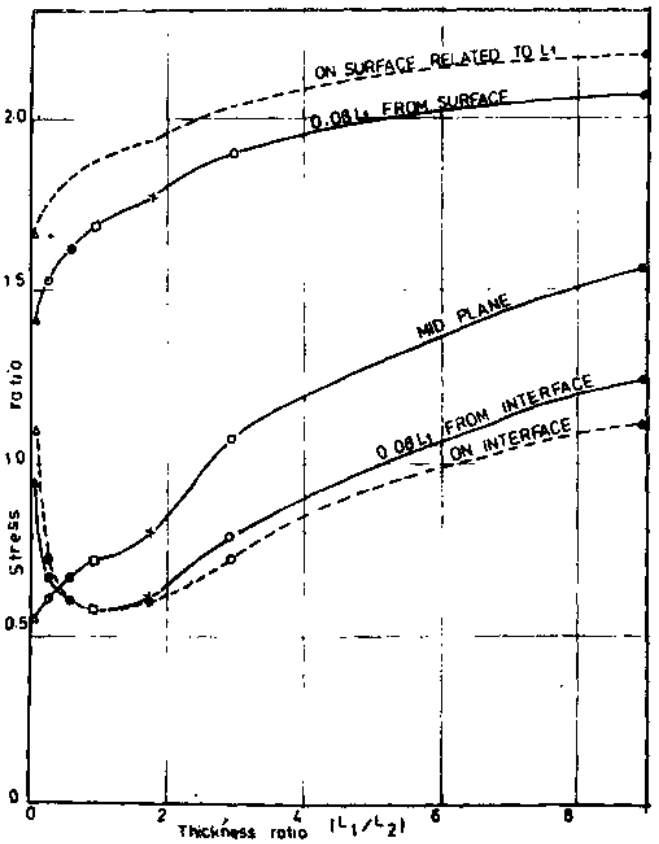

Fig. 12 Maximum stress as affected by plate thickness ratio (at .0625 *D/d* from bolt hole)

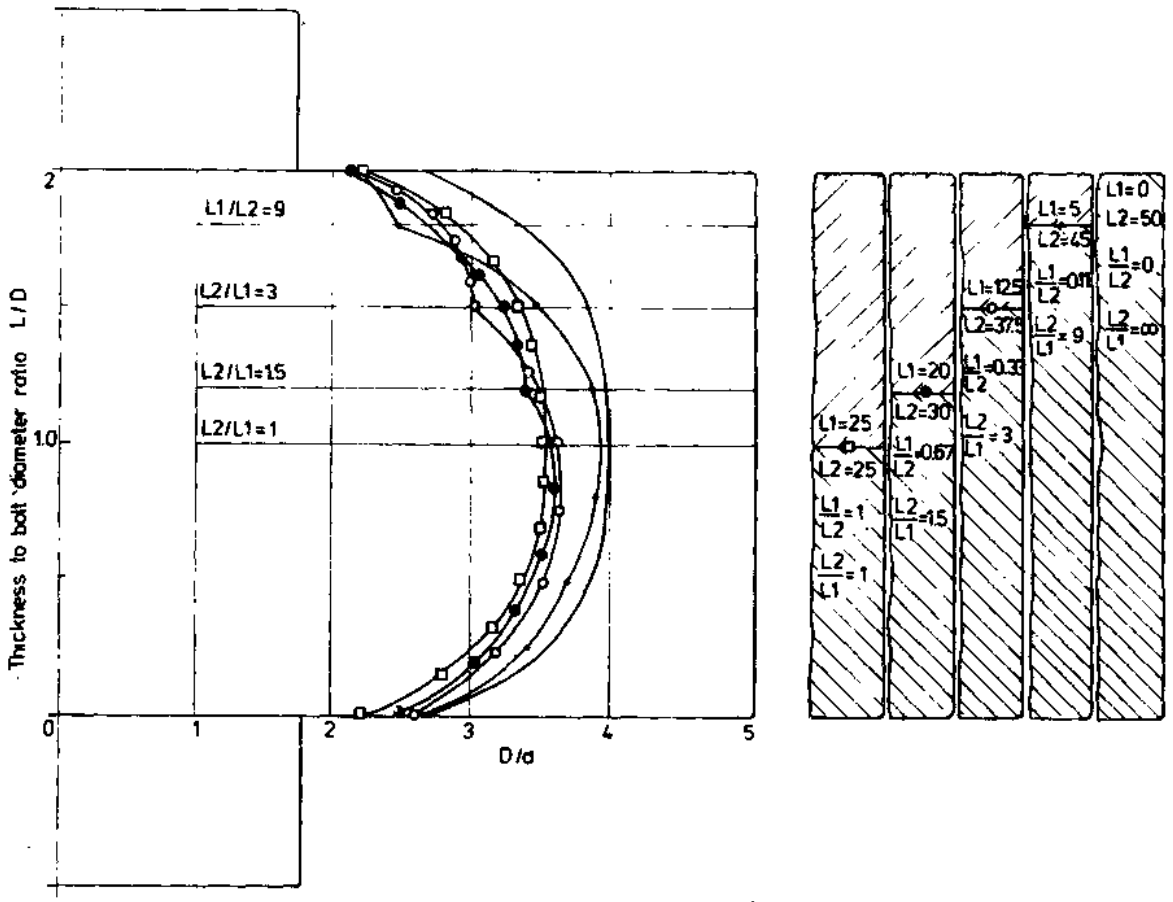

Fig. 13 End of load across joints with various thickness ratio

thickness ratio to reach its maximum value on solid plate having the same thickness of both plates. This result indicates that presumed assumption that the force is transmitted from the bolt-head and nut to the joint parts along cones of influence [9, 10] will be subject to serious errors. Further work is required to find more acceptable representations.

Conclusion

It is clear from results that the load as well as the stress or pressure distribution under bolt-head or nut are not constant nor uniform. Whatever the thickness ratio of the two plates L_1/L_2, constant load and stress are occurred across the joint under the bolt-head end. The maximum stress on interface decreases with increase in thickness ratio reaches its lowest value at $L_1/L_2 = 1$.

End of loading on surface or at mid plane increases with the increase in thickness ratio, and tends to approach a constant value at L_1/L_2 10. On interface, the opening position represented by separation radii increases with increase in thickness ratio L_1/L_2 and reaches to its maximum value of 3.5 at $L_1/L_2 = 1$ then decreases rapidly to approach a constant value of 2.5 for $L_1/L_2 \geq 10$. Also the thickness of the thinest plate L_1 has a pronounced effect on the opening position.

The effort area - boundary of end of loadings across joint increases with the increase in thickness ratio to reach its maximum value for a solid plate having the same thickness of bolt plates, hence, presumed assumption that the force is transmitted from the bolt-head to joint parts along cones of influence is no more acceptable.

References

1 Gould, H. H., and Mikic, B. B., "Areas of Contact and Pressure Distribution in Bolted Joints," ASME, Aug. 1972.

2 Motosh, N., "Stress Distribution in Joints of Bolted or Riveted Connections," ASME, *Journal of Engineering for Industry*, Feb. 1975.

3 Fernlund, I., "A Method to Calculate the Pressure Between Bolted or Riveted Plates," *Transactions of Chalmers University of Technology*, Gothenburg, Sweden, No. 254, 1961.

4 Green-Wood, J. A., "The Elastic Stresses Produced in the Mid Plane of a Slab by Pressure Applied Symmetrically at its Surface," *Proceedings of the Cambridge Philosophical Society*, England, Vol. 60, 1964.

5 Lardner, T. J., "Stresses in a Thick Plate with Axially Symmetric Loading," ASME, *Journal of Applied Mechanics*, Vol. 23, June 1965.

6 Ziada, H. H., and Abd El Latif, A. K., "Load Pressure Distribution and Contact Area in Bolted Joints," in press.

7 Zienkiewiez, O. C., *The Finite Element Method in Engineering Science*, McGraw- Hill, 1971.

8 Przemieniecki, T. S., *Theory of Matrix Structural Analysis*, McGraw-Hill, New York, 1968.

9 Motosh, N., "Determination of Joint Stiffness in Bolted Connections," *Bulletin of Assiut University*, Faculty of Engineering, Egypt, 1973.

10 El Hadidy, A. F., Abd El Latif, A. K., El- Wahi, S.E-D.H., and El Sherif, F. S., "Stiffness of Bolted Joints With and Without Gaskets," *Bulletin of Assiut University*, Faculty of Engineering, Egypt, 1978.

Printed in U.S.A.

此为试读,需要完整PDF请访问: www.ertongbook.com

ASME

Finite Element Analysis of Hydraulic Cylinders

N. Ravishankar

Structural Engineer,
U.S. Engineering Co.,
Joplin, Mo. 64801

A method of analysis which permits the investigation of stresses and deflections in a hydraulic cylinder, using a finite element analytical model, is presented. The hydraulic cylinder is modeled as an assemblage of space frame elements with a fictitious rotary spring at the gland to consider the effect of seals and bearings at the rod-cylinder interface.

Introduction

Hydraulic cylinders are the most common actuators in fluid power systems. In addition to working as fluid power components, they are required to function as structural members as well and consequently need to be designed to meet specified structural requirements. The successful performance of the hydraulic cylinder as a load carrying unit is governed by the necessity that the stresses and deflections produced at any particular load be less than tolerable limits. As axial compression is the most predominant load system, the possibility of buckling must also be examined.

Until recently, certain empirical formulas and numerous simplifying assumptions were made in hydraulic cylinder design. The assumptions range from considering the hydraulic cylinder to be a slender circular column with a radius equal to that of the rod region to assuming the cylinder to be a stepped column. The buckling loads appropriate for these simple systems were the basis of design. Of late, however, methods for including the flexibility at the interface of the cylinder and the rod due to the presence of seals and bearings and the corresponding reduction in the load carrying capacity have been developed [1].

In the earlier analyses, the solutions were obtained by resulting to conventional, closed form, differential equations and the applicability was restricted to limited boundary and loading conditions.

The purpose of this paper is to present an analytical procedure for the analysis of hydraulic cylinders under generalized loading and end conditions.

Brief Critique on Earlier Work. Early investigations [2] of hydaulic cylinders was based on the assumption that the cylinder would always fail by buckling of the rod and that the cylinder portion is infinitely stiff. Later investigators [3, 4] realized that the hydraulic cylinder can be idealized as a stepped column.

The hydraulic cylinder can be considered as a stepped column only for buckling analysis. The stepped column analysis cannot be used to determine stress failure of the cylinder, since the stress distribution in the stepped column and hydraulic cylinder differ in cylinder portion. Because of internal fluid pressure, the cylinder portion is subjected to hoop stresses which are absent in stepped columns.

The presence of compressible seals and bearings at the interface renders the hydraulic cylinder more flexible than the stepped column. Under the effect of axial load, the cylinder deflects and lateral loads perpendicular to the axis of the cylinder act on the bearings and seals. These forces transfer moments across the interface and develop a crookedness angle between the cylinder and the rod (Fig. 1). The crookedness angle interacts with the axial load to increase the deflections, moments and stresses [5] and hence reduces the load carrying capacity. In the above mentioned reference, the bearings and seals were modeled as linear springs and a moment crookedness angle relation was developed.

Although the more complete procedure [1] for dealing with the crookedness angle effect permits a consideration of wide variety of loading and support conditions, it is restricted to loading and support eccentricities only in the plane of cylinder self-weight.

Buckling of Hydraulic Cylinders. In the earlier analyses, it was assumed that the cylinder had not reached its critical load as long as the stresses in any part of the cylinder did not exceed a prescribed (allowable) stress value. This is based on a tacit rationale that as long as the stresses were below an allowable stress value, a stable equilibrium existed between the internal and external forces. In judging the axial load carrying capacity of the hydraulic cylinder, it is not only necessary to avoid a certain stress value by an adequate margin but also of preventing the occurrence of unstable equlibrium, i.e., buckling.

For purposes of this paper, the critical load will be defined as that which results in specified stresses or buckling when the cylinder is in a fully extended position.

Method of Analysis. In order to define a method sufficiently general to handle a wide variety of parameters, it is necessary to represent the hydraulic cylinder by a model which has geometric and response characteristics, as close to the original structure as possible.

In the present study the model is composed of space frame elements, each having eight degrees of freedom. The physical properties of these elements correspond to the particular region of the hydraulic cylinder they represent. The crookedness angle is taken into account by introducing a fictitious rotary spring at the junction of the rod and the cylinder.

Contributed by the Design Engineering Division for presentation at the Design Engineering Conference and Show, Chicago, Ill., March 24–27, 1980 of the AMERICAN SOCIETY OF MECHANICAL ENGINEERS. Manuscript received at ASME headquarters Dec. 17, 1979. Paper No. 80-DE-3.

Discussion on this paper will be accepted at ASME Headquarters until May 24, 1980

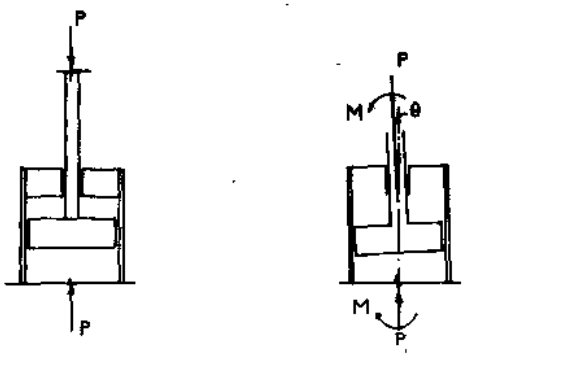

(a) STRAIGHT CYLINDER (b) DEFLECTED CYLINDER

Fig. 1 Crookedness angle

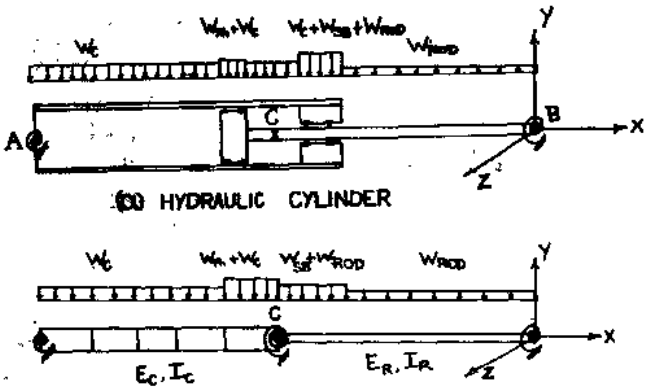

(b) FINITE ELEMENT MODEL

Fig. 2 Analytical model

In conventional finite element analysis, the displacement characteristics are assumed and the accuracy of the solution improves with a reduction in element size. However, in the present study, because the force-displacement characteristics are derived from the differential equations governing the bending of beams subjected to axial and lateral loads, the minimum number of elements necessary to represent the geometry of the hydraulic cylinder give an accurate solution.

Assumptions. The assumptions used in the development of the analysis are as follows:

(1) All materials are linearly elastic, isotropic, and homogeneous.
(2) Deflections are small compared to the length of the cylinder.
(3) The axes of the cylinder and the rod are co-linear before loading.
(4) The rod is fully extended but the piston is not in contact with the stuffing box.
(5) The length of the stuffing box is small compared to the length of the cylinder.
(6) The rod and cylinder portions comprising the interface remain straight.
(7) The bearings and seals at the sliding connection can be replaced by piecewise linear springs.
(8) There is no axial force transfer through friction in either the piston head or the stuffing box bearings.
(9) Cylinder supports can be anywhere along the length of the cylinder. However, the sliding connection must be between the cylinder and the rod supports.
(10) The system is not subjected to torsion.

Analytical Model

The assumptions discussed above permit the hydraulic cylinder to be modeled as shown in Fig. 2(*a*). Point *C* is the location at which the cylinder and the rod axis intersect when the cylinder is in a deflated position. The portion of the system to the left of *C* is considered to possess the characteristics of the cylinder portion and that to the right is treated as a part of the rod. The self-weight is assumed to act in the negative *Y* direction. The bearings and seals in the gland region are modeled as linear springs as described in [1].

The supports at the end of the cylinder can either be pinned (permit free rotation about the *Y* or *Z* axes) or fixed. For illustrative purposes only two supports have been shown in Fig. 2(*a*). However, any number of supports can be included in the analysis.

The finite element model shown in Fig. 2(*b*) represents the cylinder shown in Fig. 2(*a*). The cylinder and the rod are

Nomenclature

A = area of cross section
$[C]$ = crookedness angle matrix
E_c = modulus of elasticity of cylinder material
E_R = modulus of elasticity of rod material
e_{cy} = eccentricity at cylinder end along *Y* axis
e_{cz} = eccentricity at cylinder end along *Z* axis
e_{ry} = eccentricity at rod end along *Y* axis
e_{rz} = eccentricity at rod end along *Z* axis
$[F]^i$ = nodal force matrix
I = moment of inertia of the element
$[K]^i$ = stiffness matrix of element *i*
$K_{ij}^a K_{ij}^a K_{ji}^a K_{jj}^a$ = partioned submatrices of element *a*
L = length of the element
M_{ry} = moment at the rod end about *Y* axis
M_{rz} = moment at the rod end about *Z* axis
M_{cy} = moment at the cylinder end about *Y* axis
M_{cz} = moment at the cylinder about *Z* axis
$(M_y)_j^i$ = moment about *Y* axis at the *j*th node of the *i*th element
$(M_z)_j^i$ = moment about *Z* axis at the *j*th node of the *i*th element
P = axial load in the element
R, S, T = stiffness coefficients
$(V_y)_j^i$ = shear force along *Y* axis at the *j*th node of *i*th element
$(V_z)_j^i$ = shear force along *Z* axis at the *j*th node of *i*th element
$(v)_j^i$ = translation along the *Y* axis at the *j*th node of *i*th element
$(w)_j^i$ = translation along *Z* axis at the *j*th node of the *i*th element
w_c = weight of cylinder/unit length
w_{ph} = weight of piston head/unit length
w_{rod} = weight of rod/unit length
w_{sb} = weight of stuffing box/unit length
X, Y, Z = direction of the coordinate axes
θ_c = crookedness angle in the bending plane
ρ_j^i = rotation about *Y* axis at the *j*th node of the *i*th element
ρ_c = component of crookedness angle along *Z* axis
β_j = rotation about *Z* axis at the *j*th node of the *i*th element
β_c = component of the crookedness angle along *Y* axis

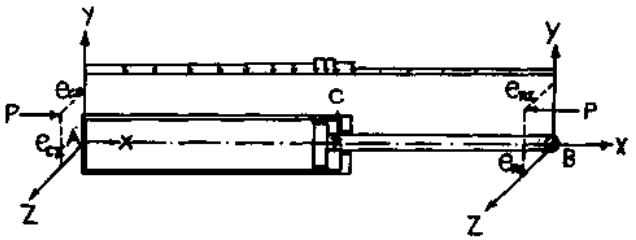

(a) ORIGINAL SYSTEM OF FORCES

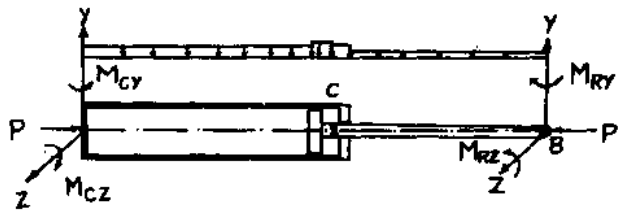

(b) EQUIVALENT SYSTEM OF FORCES

Fig. 3 Equivalent force system

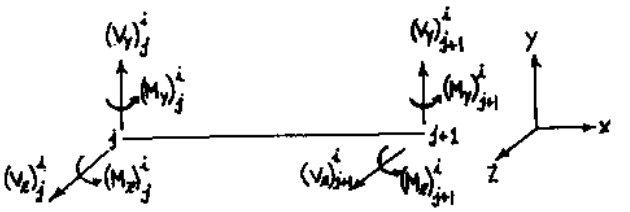

(a) MEMBER END FORCES

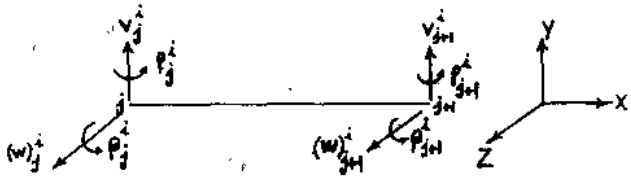

(b) MEMBER END DISPLACEMENTS

Fig. 4 Forces and displacements in a beam element

treated as one-dimensional space frame elements. The effect of the crookedness angle is taken into account by introducing a rotary spring at point C.

Method of Analysis. The present study includes the analysis of hydraulic cylinders subjected to axial loads acting at arbitrary eccentricities, as shown in Fig. 3(*a*). For the purposes of analysis the eccentric load is replaced by an equivalent system of axial load P and moments M_{RY}, M_{RZ}, M_{cy}, and M_{cz}, as shown in Fig. 3(*b*).

As discussed earlier, the model of the hydraulic cylinder is a stepped beam-column composed of space frame elements with a flexible joint at the sliding connection. Each node of the model has four degrees of freedom, restraint conditions, and forces. The sliding connection of the hydraulic cylinder is modeled as a combination of a cylinder element and a rod element separated by a fictitious rotary spring.

To begin the solution procedure, an initial value of the crookedness angle is estimated. In the case of nonvertical cylinders the initial crookedness angle is due to the self-weight moments, and in vertical cylinders an initial value is assumed. The crookedness angle so determined may be in an arbitrary bending plane and is resolved into components about the Y and Z axes. The crookedness angle produces additional forces at the gland and, hence, additional deflection. Consequently, due to the interaction of the axial load with the deflection, the moment distribution along the hydraulic cylinder length and the moment acting at the gland are changed. The moments at the gland so calculated will be about reference axes Y and Z. These moments are added vectorially to determine the interface moment in the bending plane and a new estimate of the resultant crookedness angle is calculated. The process is continued until values of the crookedness angle, obtained from successive iterations, agree to a prescribed tolerance.

After a constant value of the crookedness angle is obtained from successive iterations, the maximum stresses and deflections in the cylinder and the rod are calculated and compared with prescribed limiting values. If the calculated stresses are below the limiting values, the axial load is incremented until limiting conditions are reached.

Thus the process involves a dual iterative approach to calculate a constant value of crookedness angle for a particular axial load and to find the value of the axial load at which the stresses and deflections are very close to the tolerable limits.

Element Stiffness Matrix

The model of the cylinder is an assemblage of space frame elements, and conventional matrix analysis techniques are applied to determine the displacements and forces in the model.

Fig. 4(*a*) shows the forces acting on a single element of the structure. V_y and V_z are shear forces in the Y and Z directions. M_y and M_z are moments about the Y and Z axes, respectively. Fig. 4(*b*) shows the displacements v and w in the Y, Z directions, along with the rotations ρ and β about the Y and Z axes, respectively. The subscripts in the figure correspond to the node numbers and the superscripts correspond to the element numbers. The force-displacement relation for an element is given by

$$\{F\}^i = [K]^i\{u\}^i + \{FEM\}^i \tag{1}$$

where

$\{F\}$ = nodal force matrix;
$\{u\}$ = nodal displacement matrix;
$[K]$ = stiffness matrix of a space frame element considering the nonlinear effects of axial load.
$\{FEM\}$ = fixed end moments.

The equation (1) is expressed in matrix form as shown in Fig. 5 (equation 3).

The stiffness coefficients are in terms of R, S, T, and C where

$$R = \frac{4EI}{L^2}[K(1+C)]$$

$$T = \frac{4EI}{L^3}\left[2K(1+C) - \frac{\phi^2}{4}\right]$$

$$K\left(\frac{4EI}{L}\right) \tag{2}$$

which are in terms of

$$\phi^2 = \frac{PL^2}{EI}$$

$$K = \frac{3\lambda^2}{4\lambda^2 - \alpha^2}$$

$$C = \frac{\alpha}{2\lambda}$$

$$
\begin{bmatrix} (V_y)^j_j \\ (M_y)^j_j \\ (V_z)^j_j \\ (M_z)^j_j \\ (V_y)^j_{j+1} \\ (M_y)^j_{j+1} \\ (V_z)^j_{j+1} \\ (M_z)^j_{j+1} \end{bmatrix} = \begin{bmatrix} T & 0 & 0 & R & -T & 0 & 0 & R \\ 0 & S & -R & 0 & 0 & CS & R & 0 \\ 0 & -R & T & 0 & 0 & -R & -T & 0 \\ R & 0 & 0 & S & -R & 0 & 0 & CS \\ -T & 0 & 0 & -R & T & 0 & 0 & -R \\ 0 & CS & -R & 0 & 0 & S & R & 0 \\ 0 & R & -T & 0 & 0 & R & T & 0 \\ R & 0 & 0 & CS & -R & 0 & 0 & S \end{bmatrix} \begin{bmatrix} v^j_j \\ \rho^j_j \\ w^j_j \\ \beta^j_j \\ v^j_{j+1} \\ \rho^j_{j+1} \\ w^j_{j+1} \\ \beta^j_{j+1} \end{bmatrix} + \begin{bmatrix} \frac{ql}{2} \\ 0 \\ 0 \\ \frac{ql^2}{2} - \frac{ql^2}{2\Delta_c}(2\mathrm{Sin}\phi - \phi\mathrm{Cos}\phi - \phi) \\ \frac{ql}{2} \\ 0 \\ 0 \\ \frac{ql^2}{2\phi}\mathrm{Sin}\phi - \frac{ql^2}{\phi^2} + \frac{ql^2}{2\Delta_c}(2\mathrm{Sin}\phi - \phi\mathrm{Cos}\phi - \phi)\mathrm{Cos}\phi \end{bmatrix} \tag{3}
$$

Fig. 5 Stiffness relationship for the single element

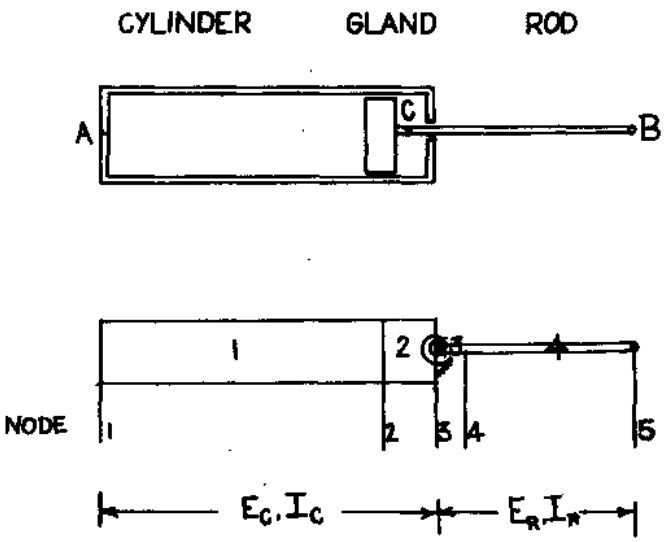

Fig. 6 Finite element model of the hydraulic cylinder

$$\lambda = \frac{3(1-\phi\cot\phi)}{\phi^2}$$

$$\alpha = \frac{-6(1-\phi\,\mathrm{cosec}\,\phi)}{\phi^2}$$

$$\Delta_c = \phi(2 - 2\cos\phi - \phi\sin\phi)$$

Determination of the Crookedness Angle

As discussed earlier, the crookedness angle reduces the load carrying capacity of the hydraulic cylinder; hence, it is necessary to understand the moment-crookedness angle relationship at the sliding connection. In the present study, the crookedness angle relationship is based on the method followed by Seshasai [1].

The crookedness angle is a function of the material properties of the bearings and seals and the geometry of the interface. As the cylinder deflects, the moment at the gland as well as the lateral forces acting on the bearings and seals increase. Because of the lateral forces, the seals and bearings are compressed and a crookedness angle develops at the sliding connection.

With an increase in the gland moment, a contact point may occur either at the front edge of the piston head or at the outside edge of the stuffing box, at which time the relationship between the moment and the crookedness angle changes. The contact point introduces a kinematic constraint and a lateral force is developed at the point of contact. The occurrence of the contact point is dependent upon clearances between the piston head and the cylinder wall, and between

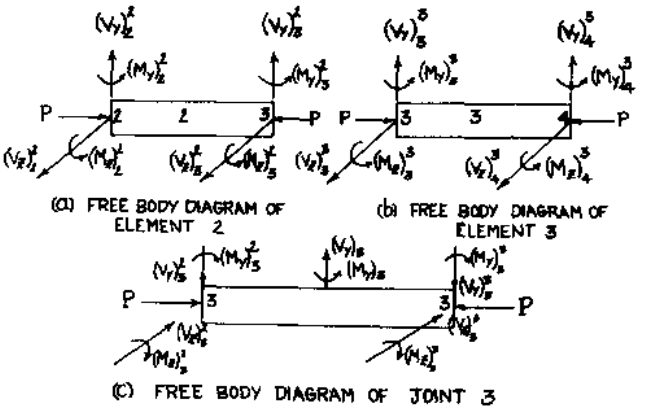

Fig. 7 Forces acting at the gland

the stuffing box and the rod as well as the lengths of the piston head, the stuffing box, and the sliding connection.

With an increase in the load, the moment at the gland increases and a second contact point may occur. The crookedness angle becomes constant after the occurrence of two contact points. Depending upon the configuration of the sliding connection, pairs of contact points may occur in three different combinations, such as the outside and inside edges of the stuffing box, the front edge of the piston head and the stuffing box, or the front and back edges of the piston.

Constraint Equations at the Gland

A simple finite element model of the hydraulic cylinder is shown in Fig. 6. Elements 1 and 4 represent the cylinder and the rod, respectively, and elements 2 and 3 together constitute the gland. The point *C* (joint 3) corresponds to the location at which the cylinder and the rod axes intersect. Elements 2 and 3 are assumed to be parts of the cylinder and the rod, respectively, and have corresponding stiffness properties.

The purpose of developing the constraint equation is to incorporate the effect of the crookedness angle at the gland. The forces acting at the gland are shown in Fig. 7. Displacements v, ρ, w, β correspond to forces V_y, M_y, V_z and M_z respectively. Superscripts on the forces and displacements in Figs. 6 and 7 correspond to element numbers and subscripts correspond to node numbers.

At *C*, due to the crookedness angle there is a discontinuity of rotation between the cylinder and the rod. In other words, at *C* the relationships between the displacement of nodes 2 and 3 are

$$\begin{aligned} \rho^2_3 &= \rho^3_3 - \rho_c \\ \beta^2_3 &= \beta^3_3 - \beta_c \\ v^2_3 &= v^3_3 \\ w^2_3 &= w^3_3 \end{aligned} \tag{4}$$

where ρ_c and β_c are components of the crookedness angle about the Y and Z axes, respectively.

From Fig. 7, equilibrium of joint 3 can be expressed as

$$\begin{aligned}(V_y)_3^2+(V_y)_3^3&=(V_y)_3\\(M_y)_3^2+(M_y)_3^3&=(M_y)_3\\(V_z)_3^2+(V_z)_3^3&=(V_z)_3\\(M_z)_3^2+(M_z)_3^3&=(M_z)_3\end{aligned}\tag{5}$$

By partitioning the stiffness matrix of elements 2 and 3, the force-displacement relationship can be expressed respectively as

$$\begin{bmatrix}K_{22}^2 & K_{23}^2\\ K_{32}^2 & K_{33}^2\end{bmatrix}\begin{bmatrix}U_2^2\\ U_3^2\end{bmatrix}=\begin{bmatrix}F_2^2\\ F_3^2\end{bmatrix}\tag{6}$$

$$\begin{bmatrix}K_{33}^3 & K_{34}^3\\ K_{43}^3 & K_{44}^3\end{bmatrix}\begin{bmatrix}U_3^3\\ U_4^3\end{bmatrix}=\begin{bmatrix}F_3^3\\ F_4^3\end{bmatrix}\tag{7}$$

where $\{U\}$ and $\{F\}$ are the displacements and forces respectively. The superscripts denote the node numbers and subscripts denote the left and the right nodes of the element.

A combination of equations (5-7) results in

$$K_{32}^2U_2^2+K_{33}^2U_3^2+K_{33}^3U_3^3+K_{34}^3U_4^3=F_3\tag{8}$$

$$K_{43}^3U_3^3+K_{44}^3U_4^3=F_4\tag{9}$$

Application of slope-compatibility relation (4) allows the joint equilibrium conditions (8, 9) to be expressed as:

$$[K_{32}^2]\{U_2\}+[K_{23}^2+K_{33}^3]\{U_3\}+[K_{34}^3]\{K_4\}=\{F\}_3-[K_{33}^2]\{C\}\tag{10}$$

$$[K_{43}^3]\{U_3\}+[K_{44}^3]\{U_4\}=\{F\}_4-[K_{43}^3]\{C\}\tag{11}$$

where $\{U_1\}$, $\{U_2\}$ and $\{U_3\}$ are nodal displacements, $\{C\}$ is the crookedness angle as denoted by a matrix

$$\{C\}=\begin{Bmatrix}0\\ \rho_c\\ 0\\ \beta_c\end{Bmatrix}$$

Equations (10) and (11) are the constraint equations of the gland, which form a part of the overall force-displacement relation.

A detailed derivation of these equations is given in reference [6].

Failure of the Cylinder. Failure in hydraulic cylinders can occur due to excessive axial stress, excessive hoop stress, a combination of axial, bending and hoop stresses resulting in excessive shear stresses or due to buckling.

The critical load of a hydraulic cylinder is reached when the stress at any point reaches a prescribed limit. The stresses to be compared with limit values are:

(1) Maximum hoop stress in the cylinder (and in the rod for pressurized rods.

(2) The shear stress at the point of maximum bending moment.

(3) The longitudinal stress due to the combination of axial load and bending moments at the extreme fibres at the point of maximum bending moment.

The failure due to buckling of the hydraulic cylinder is characterized by the load at which the force-displacement relation is numerically unstable.

Summary

A summary of the overall analysis is as follows:

(1) The hydraulic cylinder is divided into a number of finite elements.

(2) The initial crookedness angle is estimated.

(3) Stiffness matrices for each element are generated.

(4) The overall stiffness matrix is assembled.

(5) The solution of simultaneous equations is performed to calculate model dispacements.

(6) Interface moments in Y and Z directions are calculated and added vectorially to calculate the interface moment in the bending plane.

(7) The crookedness angle and its components are calculated.

(8) The position of step point C is calculated.

(9) The overall stiffness matrix is modified and steps 5 through 8 are repeated till the crookedness angle converges.

(10) Stresses, deflections and stability of the cylinder are checked.

(11) If the above values are below the allowable level and if the cylinder is stable, the axial load is incremented. Steps 3 throngh 11 are repeased.

(12) If the stress vulues are above the allowable value or if the cylinder underwent buckling, the design load has been reached.

The above method of analysis has been programmed in fortran language for solution on an IBM 370 Computer (7).

Acknowledgment

The author wishes to express his sincere appreciation and thanks to Dr. W. P. Dawkins, Professor of Civil Engineering, Oklahoma State University for his valuable guidance in the effort, and to Dr. E. C. Fitch, Director, Fluid Power Research Center, Oklahoma State University, for his encouragement and suport. The author also wishes to record his thanks to Dr. K. L. Seshasai for his suggestions and advice.

References

1 Seshasai, K. L., "Stress Analysis of Hydraulic Cylinders," Dissertation submitted for the degree of Doctor of Philosophy, Oklahoma State University, Stillwater, OK., May 1976.

2 Meier, J. H., "Buckling of Uniform and Stepped Columns—II," *Product Engineering*, Vol. 20, Nov. 1949, pp. 116-118.

3 Hoblit, F. M., "Critical Buckling Loads for Hydraulic Actuating Cylinders," *Product Engineering*, Vol. 21, July 1950, pp. 108-112.

4 Thompson, W. T., "Critical Load of Stepped Columns," *Journal of Applied Mechanics*, Vol. 17, June 1950, pp. 132-134.

5 Seshasai, K. L., Dawkins, W. P., and Iyengar, S. K. R., "Stress Analysis of Hydraulic Cylinders," Presented at the National Conference on Fluid Power, Chicago, IL, Oct. 21-23, 1975.

6 Ravishankar, N., "Biaxial Bending Analysis of Hydraulic Cylinders," Dissertation submitted for the degree of Doctor of Philosophy, Oklahoma State University, Stillwater, OK, May 1979.

7 Ravishankar, N., "Stress Analysis of Hydraulic Cylinders By Finite Element Method—Part I: Theoretical Development," *BFPR Journal*, Vol. 13, No. 2, Apr. 1979, pp. 153-162.

Printed in U.S.A.

此为试读,需要完整PDF请访问: www.ertongbook.com